Altered Env conformational dynamics as a mechanism of resistance to peptide-triazole HIV-1 inactivators

Shiyu Zhang[1,2,*], Andrew P. Holmes[1,*], Alexej Dick[1], Adel A. Rashad[1], Lucía Enríquez Rodríguez[4], Gabriela A. Canziani[1], Michael J. Root[5], Irwin M. Chaiken[1]

[1]Department of Biochemistry and Molecular Biology, Drexel University College of Medicine, Philadelphia, Pennsylvania; [2]School of Biomedical Engineering, Science and Health Systems, Drexel University, Philadelphia, Pennsylvania; [4]Faculty of Experimental Science, Francisco de Vitoria University, Madrid; [5]Department of Biochemistry and Molecular Biology, Thomas Jefferson University, Philadelphia, Pennsylvania.

We previously developed drug-like peptide triazoles (PTs) that target HIV-1 Envelope (Env) gp120, inhibit viral entry, and irreversibly inactivate virions. Here, we investigated potential mechanisms of viral escape from this promising class of HIV-1 entry inhibitors. HIV-1 resistance to cyclic (AAR029b) and linear (KR13) PTs was obtained by dose escalation in viral passaging experiments. High-level resistance for both inhibitors developed slowly (relative to escape from gp41-targeted C-peptide inhibitor C37) by acquiring mutations in gp120 both within (Val255) and distant to (Ser143) the putative PT binding site. The similarity in the resistance profiles for AAR029b and KR13 suggests that the shared IXW pharmacophore provided the primary pressure for HIV-1 escape. In single-round infectivity studies employing recombinant virus, V255I/S143N double escape mutants reduced PT antiviral potency by 150- to 3900-fold. Curiously, the combined mutations had a much smaller impact on PT binding affinity for monomeric gp120 (4- to 9-fold). This binding disruption was entirely due to the V255I mutation, which generated few steric clashes with PT in molecular docking. However, this minor effect on PT affinity belied large, offsetting changes to association enthalpy and entropy. The escape mutations had negligible effect on CD4 binding and utilization during entry, but significantly altered both binding thermodynamics and inhibitory potency of the conformationally-specific, anti-CD4i antibody 17b. Moreover, the escape mutations substantially decreased gp120 shedding induced by either soluble CD4 or AAR029b. Together, the data suggest that the escape mutations significantly modified the energetic landscape of Env's prefusogenic state, altering conformational dynamics to hinder PT-induced irreversible inactivation of Env.

Generating HIV-1 Resistance to PT Inhibitors

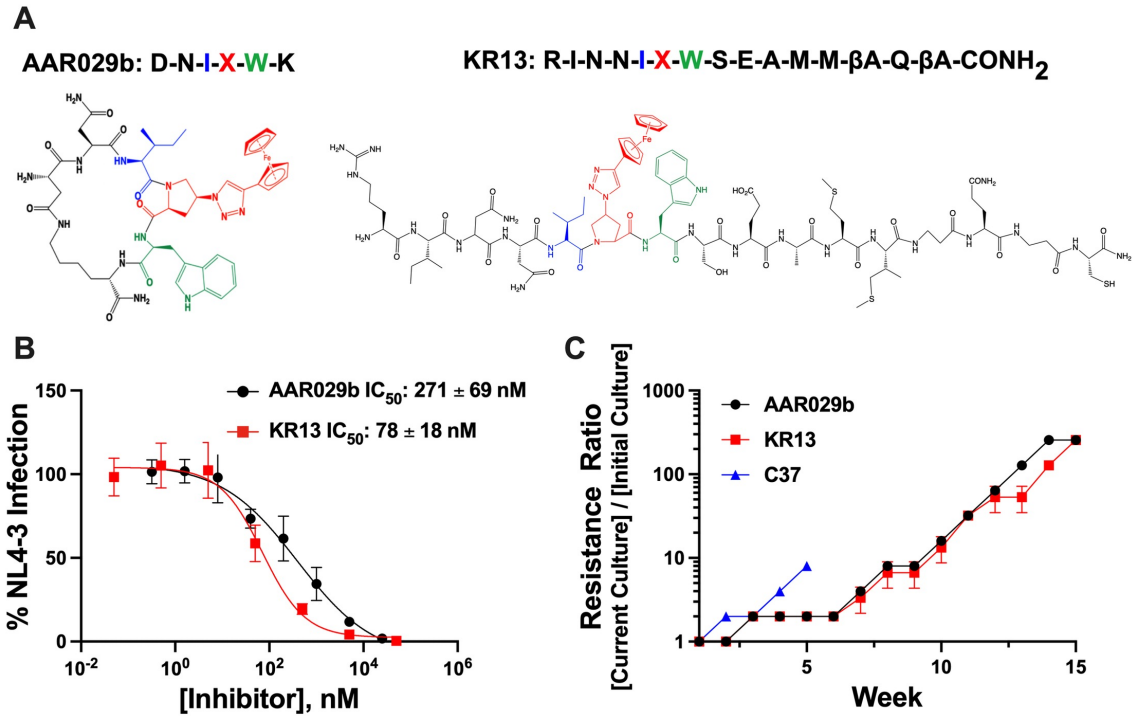

Fig 1: A. Structures of AAR029b and KR13. **B.** PT inhibitory titrations against replicating HIV-1NL4-3. Data represent the mean and standard deviation (n=3). **C.** Dose-escalation profiles of KR13 (red), AAR029b (black) and C37 (blue) used during virus passaging. C37 is a gp41-targeted fusion inhibitor with a well-defined escape profile.

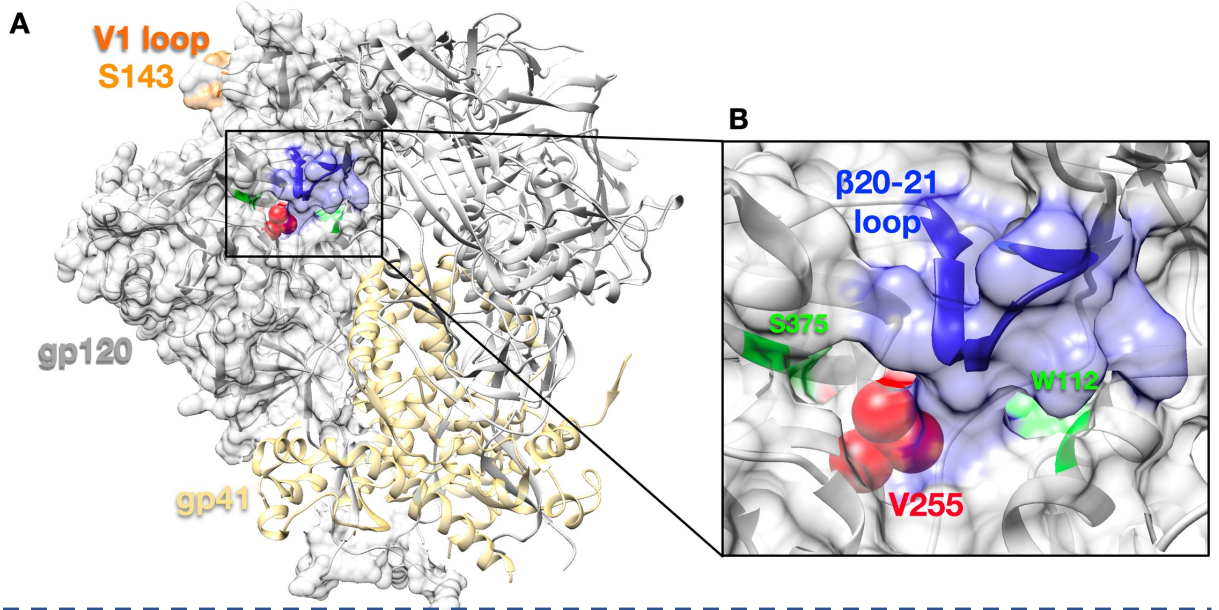

Fig 2: Location of S143 and V255 in the prefusogenic structure of a Clade B HIV-1 Env trimer (PDB: 5FUU). **A.** S143 is located in the flexible V1 loop (orange) on the apical surface while V255 (red) is located in a cavity that forms part of the putative PT binding pocket. **B.** Enlargement of the PT binding cavity showing the positions of W112 and S375 (green) that define the two subcavities of the PT binding site and the β20-21 loop (blue) that plays a critical role in Env activation.

PT Resistance Showed Greater Impact on PT Inhibition than PT Binding

	AAR029b IC_{50} (nM) (fold-change relative to WT)		KR13 IC_{50} (nM) (fold-change relative to WT)	
	NL4-3	HxBc2	NL4-3	HxBc2
Wild type	250 ± 90 (1)	230 ± 130 (1)	2.0 ± 0.56 (1)	1.2 ± 0.17 (1)
S143N	380 ± 20 (1.5)	540 ± 50 (2.3)	3.5 ± 1.5 (1.8)	1.4 ± 0.24 (1.2)
V255I	$7.6\times10^4 \pm 1.6\times10^4$ (300)	$1.4\times10^4 \pm 810$ (50)	120 ± 18 (62)	91 ± 23 (77)
V255T	$9.1\times10^4 \pm 3.9\times10^4$ (370)	$1.5\times10^4 \pm 1.5\times10^4$ (62)	360 ± 35 (180)	330 ± 70 (280)
V255I/S143N	$2.0\times10^5 \pm 2.6\times10^4$ (790)	$3.4\times10^4 \pm 2.9\times10^4$ (150)	3700 ± 560 (1900)	4600 ± 510 (3900)
V255T/S143N	$2.4\times10^5 \pm 2.7\times10^4$ (980)	$3.7\times10^4 \pm 1.8\times10^4$ (160)	6200 ± 320 (3100)	7100 ± 1100 (6000)

Table 1. Inhibitory properties of AAR029b and KR13 against HIV-1 WT and resistant pseudotyped viruses. The data indicate that the major determinant of PT resistance is residue 255. The impact of the S143N mutation was dependent on the amino acid at residue 255.

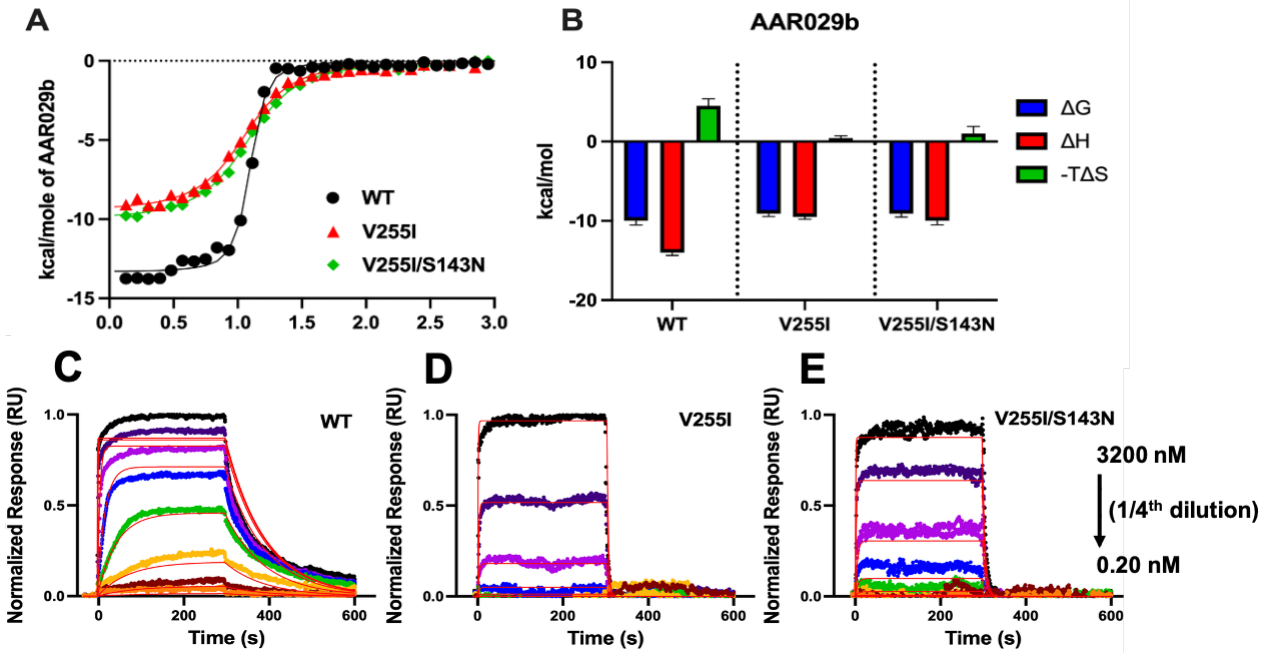

Fig 3: Thermodynamic (A-B) and kinetic (C-E) analysis of AAR029b binding to wild type and resistant gp120 by isothermal titration calorimetry (ITC) and surface plasmon resonance (SPR). The PT-induced resistance had impacts on PT binding, but milder compared the impacts on on PT neutralization.

Resistance Impact on 17b and CD4 Interaction

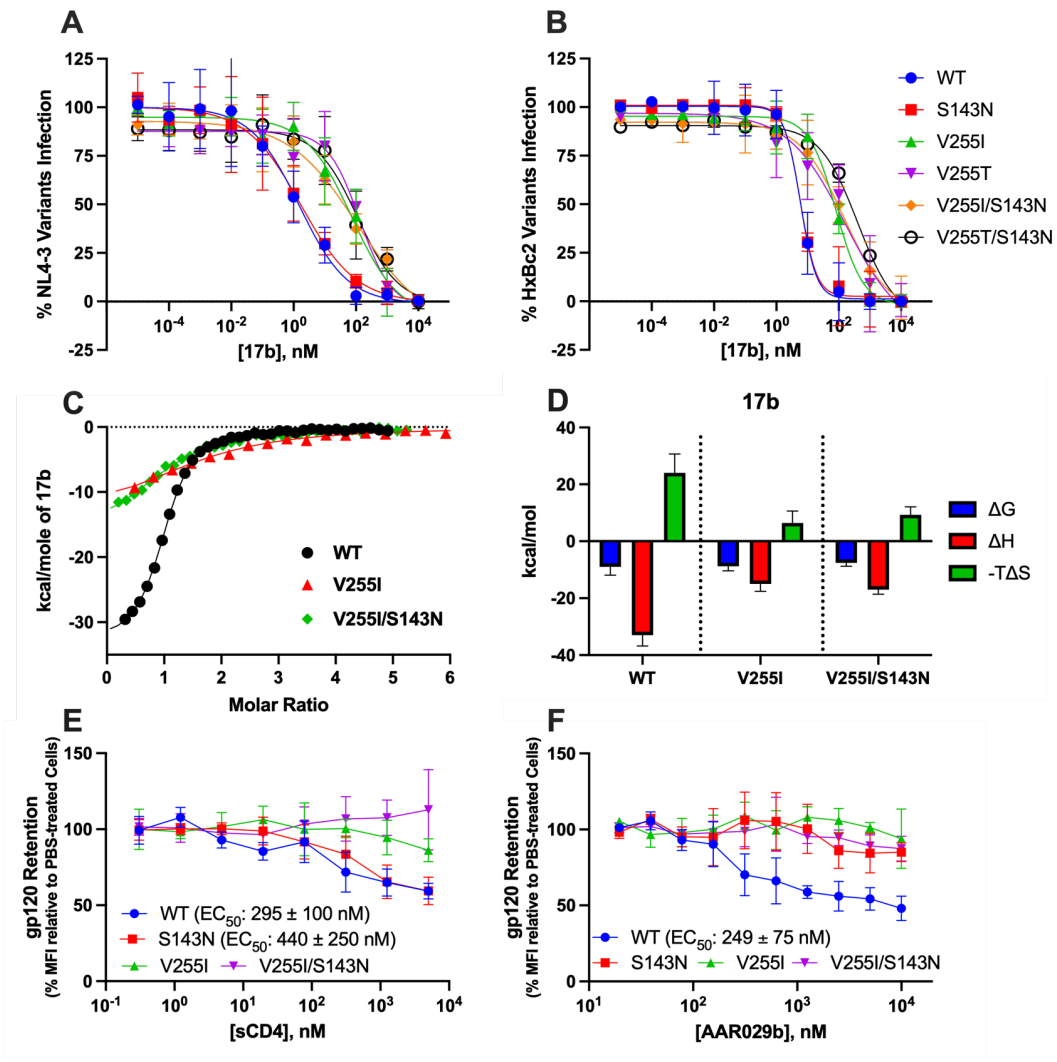

Fig 4: A-B: 17b antiviral activity against HIV-1 NL4-3 and HxBc2 strains. C-D: thermodynamic binding of 17b with gp120 monomers by ITC. E-F: CD4/PT-induced shedding detection by flow cytometry.

The results showed escape mutations affected 17b binding and inhibition, and CD4-induced interaction after its binding. The data strongly demonstrates that the escape mutations exert their binding effects by altering Env conformational dynamics including the CD4-induced inter-action after its binding and the coreceptor binding site exposure.

Proposed mechanism of PT escape

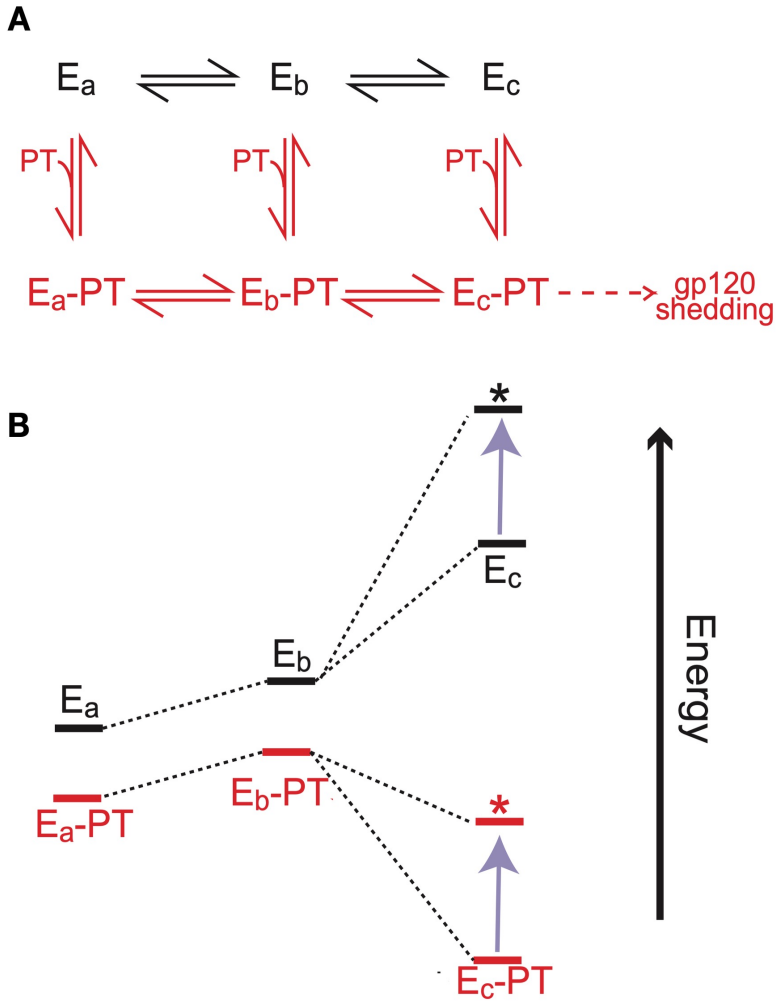

Fig 5: A. Chemical reaction scheme depicting conformational fluctuations of un-liganded and PT-bound Env in its prefusogenic state. Env is envisioned to exist in states Ea, Eb and Ec. Eb and Ec are induced by CD4 binding but only Ec possesses a fully formed bridging sheet capable of interacting with mAb 17b or coreceptor. **B. Energy levels of different con-formations of unliganded and PT-bound Env.** The effect of escape mutations on this energetic landscape is indicated by the purple arrow, where the asterisk represents the energy level of the mutated Env.

PTs can interact with all three states, but they preferentially stabilize E_c, accounting for their ability to trigger gp120 shedding. We propose that PT escape mutations selectively destabilize the E_c conformation in both the unliganded and PT-bound states. As a consequence, PT-bound Env will fluctuate more into the E_a and E_b conformations, disrupting the affinity of PT for Env as well as reducing PT-induced gp120 shedding from the E_c conformation.

Conclusion

- PT inhibitors induced resistance in slower rates.
- Similar resistance mutations arising from treatments with two PTs argue for common response to the same pharmacophore (IXW).
- Resistance mutations to the PT family occur at sites affecting both Env binding and trimer conformational organization.

Selected References

- Rashad AA, et.al. (2015) Macrocyclic Envelope Glycoprotein Antagonists that Irreversibly Inactivate HIV-1 before Host Cell Encounter. JMC.
- Aneja R, et.al. (2015) Peptide Triazole Inactivators of HIV-1 Utilize a Conserved Two-Cavity Binding Site at the Junction of the Inner and Outer Domains of Env gp120. JMC.
- Rashad AA, et.al. (2017) Expanding Chemical Space For Optimizing Macrocyclic HIV-1 Inactivators. Organic & Biomolecular Chemistry.

Acknowledgements

- This work was supported by P01GM56550/AI150471 and R01AI128815 to IMC, and by R01GM066682/AI150490 to MJR. We thank Mukta Khasnis and Koree Ahn for supporting the viral passaging studies and providing protein supplies.